

# Nonexponential Fluorescence Decay in Reaction Centers of *Rhodobacter sphaeroides* Reflecting Dispersive Charge Separation up to 1 ns<sup>†</sup>

G. Hartwich,<sup>‡</sup> H. Lossau, M. E. Michel-Beyerle,\* and A. Ogrodnik

Institut für Physikalische und Theoretische Chemie, TU München, Lichtenbergstrasse 4, D-85747 Garching, Germany

Received: October 28, 1997; In Final Form: January 20, 1998

The nonexponential fluorescence decay pattern of the primary donor state  $^1P^*$  in the reaction center (RC) of *Rhodobacter sphaeroides* R26 has been investigated in order to identify the origin of such dispersive kinetics. Of particular interest was the open question, whether “intermediate” fluorescence components ( $\approx 40$  ps to 1 ns) reflect (i) the decay of  $^1P^*$  due to slow charge separation or (ii) the thermodynamic equilibrium between  $^1P^*$  and an energetically relaxing  $P^+H_A^-$  state ( $H_A$  denoting bacteriopheophytin). Such a contribution from delayed emission of  $P^+H_A^-$  is identified by manipulating the lifetime of this state from  $\approx 100$  ps (in chinone-containing RC) to  $\approx 15$  ns (in chinone-depleted RC). The key observation is that prompt fluorescence components dominate in the time range up to  $\approx 600$  ps at 290 K since they are not affected by the  $P^+H_A^-$  lifetime. These components reflect *slow charge separation* of a minority of  $\sim 2\%$  of the RCs extending over a time window up to  $\approx 1$  ns. The distribution of charge-separation rates depends on the thermal accessibility of the radical pair  $P^+B_A^-$  and therefore mirrors energetic differences of  $P^+B_A^-$ : (i) In the majority of RCs the state  $P^+B_A^-$  is sufficiently low to ensure fast activationless charge separation ( $\approx 3$  ps), while in a minority of RCs high-lying  $P^+B_A^-$  states lead to (ii) activated, slow charge separation and to (iii) superexchange-mediated charge separation to  $P^+H_A^-$ , when  $P^+B_A^-$  is thermally no more accessible. At times longer than 600 ps the fluorescence components become sensitive to changes of the lifetime of  $P^+H_A^-$  indicating that *delayed emission* dominates. The time-dependent decrease of the delayed emission reflects an energetic relaxation of  $P^+H_A^-$  due to the conformational response of the protein to charge separation.

## 1. Introduction

One of the most characteristic kinetic features of proteins is a very pronounced nonexponentiality of a variety of processes.<sup>1,2</sup> Therefore it is not surprising that the fluorescence decay in photosynthetic reaction centers is also dispersive. It is the goal of this paper to investigate what kind of processes the different fluorescence components reflect and how they can be quantified.

Photosynthetic RCs are membrane-bound pigment–protein complexes that have a well-defined structure.<sup>3–7</sup> After optical excitation of the primary donor (P), a bacteriochlorophyll dimer, an electron is transferred to a bacteriochlorophyll monomer ( $B_A$ ), a bacteriopheophytin ( $H_A$ ), and a quinone ( $Q_A$ ) in subsequent steps.<sup>8</sup> These charge separation and the corresponding recombination reactions have been studied extensively in the last years. Early femtosecond and picosecond time-resolved measurements of the first charge-separation step were interpreted with a single time constant for the spectral transients.<sup>9–12</sup> Recent transient absorption and stimulated emission studies with improved signal-to-noise ratio as well as spontaneous emission studies reveal that the decay of the excited primary donor ( $^1P^*$ ) in RCs of *Rhodobacter sphaeroides* is nonexponential within the first 25 ps.<sup>13–16</sup> It can be characterized by two decay times ( $\sim 2$  and  $\sim 10$  ps) with relative amplitudes of about 80% and 20%.

Fluorescence measurements on a longer time scale show additional lifetime components in the time range of 40 ps to 1 ns (amplitudes  $\leq 2\%$ ) and a minor component with tens of nanoseconds (amplitude  $< 10^{-4}$ ).<sup>15,17–26</sup> Since in  $Q_A$ -depleted RCs the lifetime of  $P^+H_A^-$  is 13–40 ns and because of its characteristic dependence on temperature and magnetic field, this long-lived fluorescence component can be attributed to the  $P^+H_A^-$  recombination.<sup>23,27–30</sup>

So far, the origin of the 40 ps to 1 ns fluorescence components of  $^1P^*$  has been discussed in terms of two contributions, which reflect on specific properties of the protein: (i) The fluorescence originates from the equilibrium of  $^1P^*$  and the charge-separated state  $P^+H_A^-$ ,<sup>24,31,32</sup> which changes while the protein matrix gradually stabilizes this state. Thus, the decreasing emission amplitude monitors the relaxation of  $P^+H_A^-$  from energetically high-lying states in which it is initially formed to lower-lying states approached by the conformational response of the protein to the new charge distribution in the charge-separated state (conformational cooling). (ii) Dispersive CS has been proposed as an additional or alternative explanation for the 40 ps to 1 ns fluorescence components.<sup>17,19–21,33</sup> Accordingly these components report on slow CS processes in a minority of the RCs reflecting an inhomogeneous distribution of CS rates. Such dispersive CS is expected on the basis of an inhomogeneous distribution of driving forces for the CS step  $^1P^* \rightarrow P^+B_A^-$  induced by the natural conformational manifold.

Discarding significant contributions from slow CS to the fluorescence components exceeding 3 ps, the energy gap between  $^1P^*$  and  $P^+H_A^-$  was concluded to be several hundred  $\text{cm}^{-1}$  at room temperature and even smaller at lower temper-

<sup>†</sup> Abbreviations. RC, reaction center; *Rb. sphaeroides*, *Rhodobacter sphaeroides* R 26; P, primary donor;  $H_{A,B}$ ,  $B_{A,B}$ , and  $Q_{A,B}$ , bacteriopheophytin, monomeric bacteriochlorophyll, and ubiquinone at the A- and B-branch, respectively; OD, optical density; ET, electron transfer; CS, charge separation.

<sup>‡</sup> Current address: Gerhard Hartwich, Department of Chemical Engineering, University of Texas at Austin, Austin, TX 78712.

**TABLE 1: Multiexponential Global Fit of the Fluorescence Decay of Q<sub>A</sub>-Free and Q<sub>A</sub>-Containing RCs of *Rb. sphaeroides* R26 with Lifetimes  $\tau_i$ , Amplitudes  $a_i$ , and Relative Fluorescence Yield  $\Phi_{i,F}^{\text{rel}}$  for Each Decay Component  $i$  at 280 K ( $\chi^2_v = 1.02$ ) and 85 K ( $\chi^2_v = 1.06$ )**

| $T = 280 \text{ K}$  |         |                           | Q <sub>A</sub> -free RC |                           |  | Q <sub>A</sub> -containing RC |                           |       | $T = 85 \text{ K}$ |       |                           | Q <sub>A</sub> -free RC |                           |       | Q <sub>A</sub> -containing RC |                           |  |
|----------------------|---------|---------------------------|-------------------------|---------------------------|--|-------------------------------|---------------------------|-------|--------------------|-------|---------------------------|-------------------------|---------------------------|-------|-------------------------------|---------------------------|--|
| $\tau_i$             | $a_i^c$ | $\Phi_{i,F}^{\text{rel}}$ | $a_i$                   | $\Phi_{i,F}^{\text{rel}}$ |  | $a_i$                         | $\Phi_{i,F}^{\text{rel}}$ |       | $\tau_i$           | $a_i$ | $\Phi_{i,F}^{\text{rel}}$ | $a_i$                   | $\Phi_{i,F}^{\text{rel}}$ |       | $a_i$                         | $\Phi_{i,F}^{\text{rel}}$ |  |
| 3.5 ps <sup>a</sup>  | 10 000  | 49.9%                     | 10 000                  | 72.2%                     |  | 1.2 ps <sup>a</sup>           | 10 000                    | 13.5% | 10 000             | 15.1% |                           | 125 ps                  | 205.5                     | 28.9% | 292.1                         | 46.0%                     |  |
| 103 ps               | 69.5    | 10.2%                     | 77.9                    | 16.6%                     |  | 472 ps                        | 64.7                      | 34.4% | 63.5               | 37.8% |                           | 2.3 ns                  | 5.0                       | 13.0% | 0.3                           | 0.9%                      |  |
| 648 ps               | 13.7    | 12.6%                     | 7.5                     | 10.0%                     |  | 16.8 ns <sup>b</sup>          | 0.54                      | 10.2% | <0.01              | 0.2%  |                           |                         |                           |       |                               |                           |  |
| 3.5 ns               | 2.7     | 13.5%                     | 0.13                    | 0.9%                      |  |                               |                           |       |                    |       |                           |                         |                           |       |                               |                           |  |
| 13.3 ns <sup>b</sup> | 0.73    | 13.8%                     | <0.01                   | 0.3%                      |  |                               |                           |       |                    |       |                           |                         |                           |       |                               |                           |  |

<sup>a</sup> Literature data,<sup>13–16,46</sup> for  $T = 280 \text{ K}$  an average value of 3.5 ps for  $\tau_1 \sim 2.3 \text{ ps}$  (79%) and  $\tau_2 \sim 10 \text{ ps}$  (21%) was taken. <sup>b</sup> The longest nanosecond time constant has been obtained from a global fit of the fluorescence data collected in a time window expanded to 80 ns. <sup>c</sup> All amplitudes correspond to an amplitude of  $a_i(\tau_1) = 10\,000$  for the fastest component.

ature.<sup>18</sup> Problems imposed by such a small energy gap on the primary CS have been discussed.<sup>18,31</sup>

In this paper we utilize the possibility of manipulating the  $\text{P}^+\text{H}_\text{A}^-$  lifetime by Q<sub>A</sub> extraction and reconstitution to determine the origin of the 40 ps to 1 ns fluorescence. In the presence of Q<sub>A</sub> the  $\text{P}^+\text{H}_\text{A}^-$  lifetime is limited to  $\sim 100\text{--}200 \text{ ps}$ <sup>8,10,34–36</sup> by further CS to Q<sub>A</sub>. In the absence of Q<sub>A</sub> the electron transport chain is interrupted and  $\text{P}^+\text{H}_\text{A}^-$  lives  $\sim 10\text{--}20 \text{ ns}$  before it recombines to the ground-state P and the triplet-state  $^3\text{P}^*$ .<sup>23,27–29</sup> The central goal is to discriminate between the two contributions originating (i) from conformational cooling of  $\text{P}^+\text{H}_\text{A}^-$ , which is sensitive to changes of its lifetime, and (ii) from dispersive CS, which is independent of the  $\text{P}^+\text{H}_\text{A}^-$  lifetime. Implications of the energetic dispersion of  $\text{P}^+\text{B}_\text{A}^-$  and  $\text{P}^+\text{H}_\text{A}^-$  states on CS processes in the 100–1000 ps time range will be discussed.

## 2. Materials and Methods

**2.1. Preparation.** RCs from *Rb. sphaeroides* R26 were prepared by standard methods;<sup>37</sup> quinone extraction was achieved according to ref 38. Residual Q<sub>A</sub> content was determined according to ref 39 to be less than 1%. To optimize comparability of data from Q<sub>A</sub>-free and Q<sub>A</sub>-containing RCs, the latter samples were prepared from the same stock of Q<sub>A</sub>-free RCs by quinone reconstitution achieved by incubation with a 50-fold molar excess of ubiquinone dissolved in ethanol/dimethyl sulfoxide (1:2, 5 mg/mL) for 4 h at 0 °C. The Q<sub>A</sub> content was determined to be higher than 95%. A  $\sim 150 \mu\text{m}$  thin sample of the RCs ( $\text{OD}_{860} \sim 0.1$ ) in TL-buffer (aqueous buffer at pH = 8 containing 10 mM tris(hydroxymethyl)aminomethane and 0.1 vol % lauryl dimethylaminooxide) is sandwiched between the long sides of two rectangular prisms forming a rectangular cube. Two orthogonal faces of the cube were positioned perpendicular to the direction of excitation and fluorescence detection, orienting the film in 45° to both directions while thus minimizing refraction effects.

**2.2. Time-Resolved Fluorescence.** The fluorescence decay traces were collected with a time-correlated single-photon-counting apparatus described in ref 17. The samples were excited with a laser diode at 864 nm (Hamamatsu PLP-01, repetition rate 10 MHz, pulse energy 2 pJ, pulse width 40 ps) focused to an area of ca. 3 mm<sup>2</sup> resulting in an average turnover rate of less than  $10^{-3} \text{ s}^{-1}$ . Thus, excitation conditions are far from accumulating  $\text{P}^+\text{Q}_\text{A}^-$ . Amplified spontaneous emission in the excitation laser beams was suppressed with suitable spectral filters; the emission collected from the sample was spectrally filtered at 920 nm (Schott DAD 8-2) achieving a rejection for 864 nm stray light of  $10^{-4}$ . The fluorescence was detected with a MCP-photomultiplier equipped with a selected S1-cathode. The instrumental response function was 40 ps (full width at half-maximum, fwhm). Time constants are extracted

from the fluorescence decay pattern by fitting a convolution of the instrumental response function and the exponential decay function to the data using the Levenberg–Marquardt method.<sup>40</sup> Deconvolution of Q<sub>A</sub>-free and Q<sub>A</sub>-containing RCs at different excitation wavelengths was done simultaneously in a global analysis with *common* lifetimes and with *individual* amplitudes as free running parameters. Quality of the fit is judged by observing the residuals and values of the reduced  $\chi$ -squared.<sup>40</sup>

## 3. Results and Discussion

**3.1. Influence of Q<sub>A</sub>-Content on the Fluorescence Decay Pattern.** The lifetime of  $\text{P}^+\text{H}_\text{A}^-$  increases from 200 ps in the presence of Q<sub>A</sub><sup>8,10,34–36</sup> to  $\sim 13 \text{ ns}$  in the absence of Q<sub>A</sub>.<sup>23,27–29</sup> at room temperature and from 130 ps to  $\sim 23 \text{ ns}$  at 85 K, respectively. To discuss the influence of the lifetime of  $\text{P}^+\text{H}_\text{A}^-$  on the fluorescence decay, we discriminate three time regimes: (i) 1–20 ps prompt fluorescence components which are below our time resolution and reflect primary CS of the majority of RCs, (ii)  $\approx 50\text{--}5000 \text{ ps}$  fluorescence components (intermediate components), the origin of which is subject of this paper, and (iii) the delayed fluorescence components in the 10–20 ns region, which reflect the recombination  $\text{P}^+\text{H}_\text{A}^-$ .<sup>17,19,23–26,30</sup>

The quantification of the fluorescence decay data (Table 1) has been achieved by a global fitting procedure, assuming an identical set of time constants for both Q<sub>A</sub>-free and Q<sub>A</sub>-containing RCs, but allowing for different amplitudes. Individual fits of the various decay traces do not yield a unique set of time constants for the intermediate components, so they apparently do not represent kinetically distinct states of the system. Therefore, these time constants should rather be regarded as a description of a continuous distribution of lifetimes. For the time being the time constant for fast primary CS (fast prompt fluorescence, not resolved in our experiment) is taken to be independent of Q<sub>A</sub> content as indicated from subpicosecond studies.<sup>13</sup>

The manipulation of the  $\text{P}^+\text{H}_\text{A}^-$  lifetime by the presence or absence of Q<sub>A</sub> leads to marked differences in the fluorescence decay pattern of  $^1\text{P}^*$  (Figure 1). At 280 K (Figure 1A) the decay traces normalized to identical amplitude of the 3 ps component are almost indistinguishable within the first 300 ps and at longer times the Q<sub>A</sub>-containing sample decays more rapidly than the Q<sub>A</sub>-free sample. The global fit of the decay traces reveals that the amplitudes of the intermediate components (lifetimes of 103 and 648 ps, respectively) are almost independent of the Q<sub>A</sub> content of the sample, while the component with a 3.7 ns time constant is much more pronounced in the Q<sub>A</sub>-depleted sample than in the reconstituted one and behaves more like the slowest (13 ns) component. This component originates from delayed fluorescence of  $\text{P}^+\text{H}_\text{A}^-$  recombination in Q<sub>A</sub>-depleted RCs,<sup>17,19,23–26,30</sup> and its amplitude becomes very small when

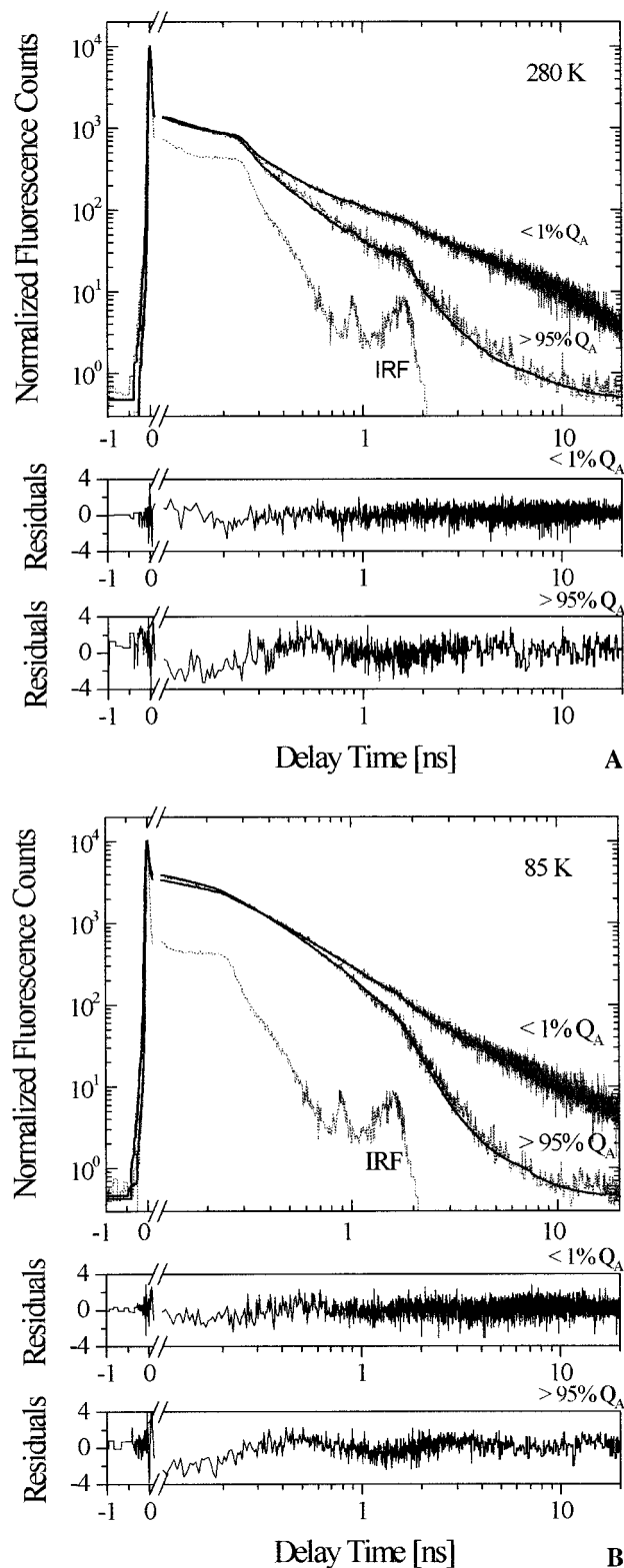


**Figure 1.** Decay of the 920 nm fluorescence of *Rb. sphaeroides* RCs excited at 864 nm in the absence and presence of  $Q_A$  recorded at (A) 280 K and (B) 85 K. Experimental data are dotted, dark gray; multiexponential fit curves (parameters are given in Table 1) are indicated by straight black lines. Note the linear time scale before (−1 to 0.1 ns) and the log time scale after x-axis break (0.1–20 ns). IRF = instrumental response function.

$Q_A$  is reconstituted. Quantitatively this finding is in good agreement with the residual  $Q_A$  content of the  $Q_A$ -depleted sample, which was determined to be less than 1%, and a content of >95% for the reconstituted one.

At 85 K (Figure 1B) the effect of the  $Q_A$  content on the fluorescence decay is similar, although the pronounced deviation is restricted to times longer than ~600 ps. The amplitudes of the intermediate components in  $Q_A$ -free RCs increase by a factor of 3–4 on lowering the temperature but remain unchanged (472 ps component) or even increase (125 ps component) upon  $Q_A$  reconstitution. The amplitude of the 2.3 ns component again behaves in a similar way as the longest time constant. Both nearly vanish upon  $Q_A$  reconstitution.

**3.2. The Intermediate Fluorescence Components Are Not Due to Sample Impurities.** The intermediate fluorescence components constitute an integral part of functional RCs isolated from the membrane. This conclusion is supported by the approximate independence of the fluorescence quantum yields of the intermediate components on sample preparation and/or detection wavelength (in the range of 900–950 nm) as well as by low-temperature (85 K) time-resolved fluorescence excitation spectra<sup>19</sup> essentially exhibiting absorption characteristics typical for native RCs. The conclusion that the intermediate components constitute an integral part of functional RCs and do not originate from sample impurities such as free pigments or inactive RCs has also been deduced by other groups<sup>18</sup> and is strengthened by the fact that these components are also found in membrane-bound RCs, which have suffered less preparational strain.<sup>41–43</sup>

**3.3. Origin of the Intermediate Fluorescence Components.** A model discarding slow CS and only considering conformational cooling was employed for  $Q_A$ -reduced RCs, and the intermediate components were exclusively assigned to solvation processes in the state  $P^+H_A^-$ .<sup>18,24,26,31,32</sup> The large number of degrees of freedom inherent in the protein matrix gradually stabilizes the charge-separated state  $P^+H_A^-$ , which initially lies close to  $^1P^*$ . While running through all possible substates  $P^+H_A^-$  eventually decreases in energy. According to this energetic relaxation process the delayed recombination fluorescence amplitude also decreases. Reconstitution of the  $Q_A$ -free RC sample with  $Q_A$  changes the lifetime of  $P^+H_A^-$  from several nanoseconds to 100–200 ps so that all delayed recombination fluorescence components from  $P^+H_A^-$  with lifetimes longer than 100–200 ps should vanish. However, little effect is seen on the detected emission.

For clarification, the decay of  $Q_A$ -free RCs relative to the decay of  $Q_A$ -reconstituted RCs is depicted in Figure 2. Independent of temperature a significant influence of  $Q_A$  reconstitution on the fluorescence decay is observed only in the nanosecond region and is most pronounced around 10 ns. At 280 K almost no influence of the  $Q_A$  content on the fluorescence decay is observable for delay times up to ~500 ps and at 85 K, where the overall contribution of the intermediate fluorescence components is more pronounced, the invariant region is even extended to ~1 ns. These observations also hold for slightly increased lifetimes  $\tau_1$  of  $Q_A$ -free RCs relative to  $Q_A$ -containing RCs.<sup>44</sup> While in the literature the primary CS rates for  $Q_A$ -free and  $Q_A$ -reconstituted RC are reported to be the same,<sup>13</sup> new fluorescence upconversion measurements<sup>45</sup> indicate a  $\tau_1$  value for  $Q_A$ -free RCs increased by ~30% relative to the mean value of published  $\tau_1$  data for  $Q_A$ -containing RCs.<sup>46–50</sup> Therefore we have varied the ratio of  $\tau_1(Q_A\text{-free RC})/\tau_1(Q_A\text{-reconstituted RC})$  in the range from 1 to 1.5.

The weak influence of the lifetime of  $P^+H_A^-$  on the intermediate fluorescence components in the time range 100 ps to 1 ns at 85 K and 200 to 500 ps at 280 K reveals that they do not represent delayed fluorescence of the state  $P^+H_A^-$ . Thus,

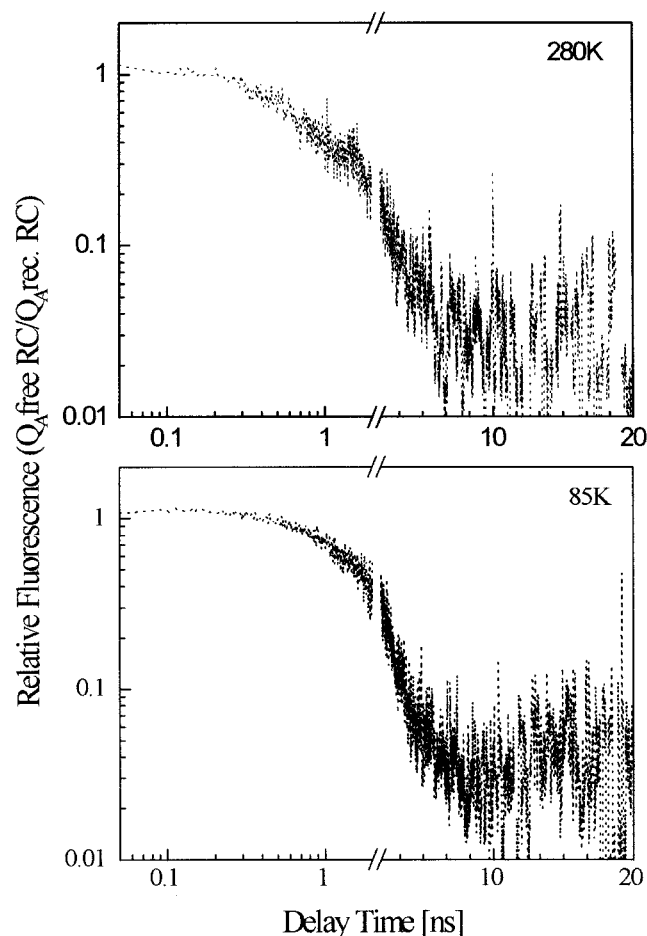


**Figure 2.** Fluorescence decay of  $Q_A$ -free RC relative to  $Q_A$ -containing RCs normalized to identical fluorescence intensity at time zero.

these components have to be prompt fluorescence reflecting slow CS processes.

The occurrence of CS on a time scale of up to several 100 ps is limited by other decay processes of the  $^1P^*$  state. The intrinsic lifetime of  $^1P^*$  in absence of CS should be dominated by internal conversion from  $^1P^*$  to the ground state and has been estimated from RC mutants  $D_{LL}$  and  $D_{LL-2a}$  mutant of *Rhodospirillum rubrum*,<sup>51</sup> which are not able to undergo primary CS. First measurements in a 200 ps time window yielded an internal conversion rate of 200 ps<sup>52</sup> and was taken as an argument against CS on the 100 ps time scale.<sup>18,31</sup> More dedicated measurements in a sufficiently long time window, however, revealed a biexponential decay with the time constants 340 and 720 ps at 260 K (440 and 840 ps at 80 K).<sup>53</sup> In chemically modified RC of *Rb. sphaeroides* R26, where we expect the least perturbation on the primary donor, the internal conversion rate was obtained from the quantum yield of  $P^+Q_A^-$  formation. In such a sample primary CS is slowed to several hundred picoseconds, so that internal conversion leads to detectable losses. An average rate of 1.1 ns at 85 K and 750 ps at 270 K<sup>54</sup> was obtained. These long intrinsic lifetimes are very well compatible with our observation of slow CS extending up to nanoseconds.

**3.4. Electric Field Effect on the Intermediate Emission Components.** Electric field effects are expected to give important information concerning charge separation, its mechanism, and its dispersion. The large electrical field induced change observed on the fluorescence of RCs<sup>20–22,55–57</sup> clearly demonstrates that a charge-separated state with large dipole moments has to be involved in this effect (e.g.,  $P^+H_A^-$  is shifted

up to 160 meV in energy at a field of  $1 \times 10^6$  V/cm). Time-resolved studies<sup>20–22</sup> show that the intermediate fluorescence components are affected almost exclusively: At 85 K the amplitude of the component around 100 ps increases by  $\sim 40\%$ , that of the component around 400 ps by  $\sim 150\%$ , and that of the component around 1–2 ns by  $\sim 400\%$ , while the unresolved fast fluorescence component experiences only changes of its emission yield of less than 10%. From the anisotropy of the electric field effect on the total (steady-state) emission it is inferred that the orientation of the relevant dipole moment is parallel to that of  $P^+H_A^-$ .<sup>56–58</sup> Since the electric field experiments have been performed on RCs typically containing about 90%  $Q_A$ , we conclude that the field effect and its orientational fingerprint refer to the prompt part of the intermediate fluorescence components. It reflects field-induced slowing of CS in this time range and reveals the prevalence of charge separation directly forming  $P^+H_A^-$ . Otherwise one would expect the dipole orientation of  $P^+B_A^-$  to determine the anisotropy. We therefore conclude that the field-sensitive charge-separation components being slower than 300 ps represent superexchange ET to  $P^+H_A^-$  mediated via the state  $P^+B_A^-$ .<sup>59</sup>

Summarizing sections 3.1–3.4, the 40 ps to 1 ns fluorescence components represent the concentration of a small subpopulation of RCs ( $<2\%$ , Table 1) whose time constants are characteristic for the long-living tail of a distribution of the primary CS rates. Thus, the distribution of primary CS rates indicated by the biexponential decay of  $^1P^*$  within the first 25 ps<sup>13–16</sup> actually extends to nanoseconds. It is known that the majority of RCs perform a sequential, activationless primary CS from  $^1P^*$  to  $P^+B_A^-$ <sup>47,48</sup> within a few picoseconds. An energetic dispersion of  $P^+B_A^-$  states leads to slow CS with increasing thermal activation. Above a certain activation barrier CS to  $P^+B_A^-$  becomes slower than superexchange-mediated CS to  $P^+H_A^-$ , which then prevails at long times.

The decay kinetics of  $^1P^*$  have been modeled recently<sup>60,61</sup> as a function of the free energy gap  $\Delta G_1$  to  $P^+B_A^-$ . Allowing for both CS channels to perform in parallel the relative contribution of sequential CS via  $P^+B_A^-$  and of superexchange CS to  $P^+H_A^-$  to the overall decay was determined. Variation of  $\Delta G_1$  within the inverted and quasi-activationless regime (from  $-500$  to  $+300$  cm<sup>-1</sup>) does not change the overall lifetimes significantly. Only at higher  $\Delta G_1$  thermal activation leads to a slowing of the  $^1P^*$  decay and an increasing contribution from superexchange CS. On the basis of this model, dispersive  $^1P^*$  decay kinetics was simulated for the case that  $\Delta G_1$  is inhomogeneously broadened<sup>61</sup> according to a Gaussian distribution with a fwhm of 0.1 eV.<sup>17</sup> Qualitatively the same picture of nonexponential decay kinetics was derived as obtained in this work. Quantitatively, however, the experimental decay components in the 100–1000 ps range are significantly larger, indicating that the shape of the distribution function deviates significantly from a Gaussian one.

It is interesting to note that time-resolved excitation spectra of the fluorescence components associated with this slow CS have a characteristic spectral fingerprint different from the bulk absorption.<sup>19</sup> The excitation spectrum of the intermediate fluorescence at 85 K, which in those experiments were represented by a 67 ps and a 342 ps component, exhibit a 230 cm<sup>-1</sup> blue shift of the 890 nm absorption maximum of P, while the fluorescence excitation spectrum of the 1.2 ps component is not shifted. Apparently there exists a correlation between the inhomogeneous broadening of the  $^1P^*$  and of the  $P^+B_A^-$  state. The blue-shifted, energetically high-lying  $^1P^*$  states face

$P^+B_A^-$  states, which have experienced an even stronger upshift in energy, so that CS slows down as observed.

**3.5. Consequences for the Energetics of  $P^+H_A^-$ .** In contrast to the fluorescence components faster than 500–1000 ps, the slower components show a strong dependence on the lifetime of  $P^+H_A^-$  (Table 1, Figures 1 and 2). This indicates that delayed emission dominates in this time window giving access to an estimation of the free energy gap between  $^1P^*$  and  $P^+H_A^-$ . In zero-order approximation we estimate this contribution by subtracting the fluorescence decay trace of  $Q_A$ -containing RCs from that for  $Q_A$ -free RC, thus essentially eliminating the prompt emission components. Instead of taking the real decay traces, which suffer from noise, we take the amplitudes of the globally fitted components and subtract them for each individual time constant  $\tau_i$  from one another, yielding  $A_i^{\text{del}}$ . Of course we can account for delayed emission only at times  $>200$  ps (at 280 K) or  $>100$  ps (at 85 K), respectively. From  $A_i^{\text{del}}$  an apparent free energy difference corresponding to the various time constants can be evaluated according to<sup>17,30</sup>

$$\Delta G_i^{\text{app}} = -k_B T \ln \frac{A_i^{\text{del}}}{A_{\text{prom}}} \quad (1)$$

$A_{\text{prom}}$  is the total amplitude of all prompt fluorescence, which in this context essentially is the amplitude of the fastest component  $a_1$ ,  $T$  is the temperature, and  $k_B$  is the Boltzmann constant. This apparent free energy difference represents an inhomogeneous distribution of  $P^+H_A^-$  energies. Assuming a Gaussian distribution with a total width of  $2\sigma$ , the center of gravity of the distribution can be estimated:<sup>17</sup>

$$\Delta G_i^0 = \Delta G_i^{\text{app}} + \frac{\sigma^2}{2k_B T} \quad (2)$$

A value of  $\sigma = 0.045$  eV was found for the slowest fluorescence component associated with the radical pair state  $P^+H_A^-$  in its lowest relaxation state, just prior to recombination.<sup>17</sup> Having no information available about the temporal evolution of  $\sigma$ , we assume  $\sigma$  to be time-independent. The resulting (time-dependent) values for the “apparent” free energy gap  $\Delta G_i^{\text{app}}$  and for the average free energy gap  $\Delta G_i^0$  between  $^1P^*$  and  $P^+H_A^-$  are listed in Table 2.

Taking identical primary CS rates in  $Q_A$ -free and  $Q_A$ -containing RCs, there is only a small temporary evolution of the free energy gap  $^1P^* - P^+H_A^-$  developing mainly on the nanosecond time scale. At high temperature an average free energy gap  $\Delta G_0$  of 0.22 eV for the first state  $P^+H_A^-$  about 300 ps after CS and a  $\Delta G_0$  of 0.27 eV for the most relaxed state  $P^+H_A^-$  is obtained. At low temperature the influence of nanosecond-solvation on the average free energy is even smaller ( $\Delta G_0$  values of initially 0.19 eV relaxing with a 2.3 ns time constant and finally 0.21 eV). Again we have varied the ratio of  $\tau_1(Q_A\text{-free RC})/\tau_1(Q_A\text{-reconstituted RC})$  in the range from 1 to 1.5 thus providing a lower limit for the energy gaps. This does not alter the  $\Delta G_0$  values for the most relaxed state  $P^+H_A^-$  and decreases  $\Delta G_0$  for the initially formed state  $P^+H_A^-$  to 0.20 eV at 280 K.

Although these energy gaps differ from  $\Delta G_0 = 0.25$  eV (as derived from magnetic field dependent recombinations dynamics after nanoseconds), the smaller values are well compatible with results from previous modeling of primary charge separation/recombination processes.<sup>60,61</sup>

However, these smaller average free energy gaps are significantly larger than those obtained without accounting for prompt

**TABLE 2: Lifetimes  $\tau_i$  and Amplitudes  $A_i^{\text{del}}$  for the Contribution of Delayed Fluorescence of  $^1P^*$  in RCs of *Rb. sphaeroides* R26 and Corresponding Values for the Apparent Free Energy  $\Delta G_i^{\text{app}}$  (Eq 1) and the Actual Free Energy  $\Delta G_i^0$  (Eq 2)<sup>a</sup>**

| $\tau_i$ [ns]    | $A_i^{\text{del}}$ <sup>b</sup> | $\Delta G_i^{\text{app}}$<br>( $^1P^* - P^+H_A^-$ )<br>[eV] | $\Delta G_i^0$<br>( $^1P^* - P^+H_A^-$ )<br>[eV] |
|------------------|---------------------------------|---|--|
| <i>T</i> = 280 K |                                 |   |  |
| 0.65             | 10.8...6.2                      | 0.163...0.181   | 0.204...0.222                                    |
| 3.5              | 3.7...2.6                       | 0.192...0.203   | 0.233...0.244                                    |
| 13.3             | 1.0...0.7                       | 0.225...0.233   | 0.266...0.274                                    |
| <i>T</i> = 85 K  |                                 |   |  |
| 0.47             | 8.6...1.2 <sup>d</sup>          | 0.053...—/— <sup>c</sup>                                    | 0.189...—/—                                      |
| 2.3              | 5.2...4.7                       | 0.056...0.057   | 0.192...0.193                                    |
| 16.8             | 0.6...0.5                       | 0.072...0.073   | 0.208...0.209                                    |

<sup>a</sup> Ranges of energy values are given corresponding to a range of  $\tau_1(Q_A\text{-free RC})$  values, with  $\tau_1(Q_A\text{-free RC})/\tau_1(Q_A\text{-containing RC}) = 1.5...0.1$  (see text). <sup>b</sup>  $A_i^{\text{del}}$  values refer to a prompt fluorescence amplitude  $A_{\text{prom}}$ , which was set equal to  $a_1(\tau_1) = 10\,000$ . <sup>c</sup> —/— the corresponding amplitude  $A_i^{\text{del}}$  turns out to be negative for  $\tau_1(Q_A\text{-free RC})/\tau_1(Q_A\text{-containing RC}) = 1$ , which either indicates that the true  $\tau_1$ -ratio is larger than 1 or that slow CS components in  $Q_A$ -free RC and  $Q_A$ -containing RCs are not identical but vary slightly. <sup>d</sup> The value of  $A_i^{\text{del}} = 1.2$  is much smaller than the error in the amplitudes indicating that a delayed fluorescence with  $\tau = 0.47$  ns cannot be verified at 85 K.

emission and thus for slow charge separation. Under this condition values as low as a few tens of millielectronvolts at room temperature and even smaller at low temperature were obtained.<sup>18,31,32,62,63</sup> Such ultrasmall free energy gaps between  $^1P^*$  and  $P^+H_A^-$  would impose severe restrictions on the driving force of the first and second charge-separation steps to  $P^+B_A^-$  and  $P^+H_A^-$ . At any rate, extremely small driving forces for the first step are in conflict with the inverse temperature dependence of the majority behavior of charge separation indicating activationless CS, as long as one allows for reasonable values of the reorganization energy. Such problems do not arise with the free energy data derived in this paper.

#### 4. Conclusions

The  $^1P^*$  fluorescence components with lifetimes of 40 ps to approximately 1 ns reflect an integral constituent of functional RCs. Their amplitudes are almost independent of the lifetime of  $P^+H_A^-$ , proving that they do not originate from recombination of energetically nonrelaxed  $P^+H_A^-$  states, but from slow primary CS in a minority of RCs. Since the majority of RCs performs an activationless, two-step CS from  $^1P^*$  to  $P^+B_A^-$  within 3 ps, a significant energetic inhomogeneity of the  $P^+B_A^-$  states is required to account for the observed slow CS events. Such an energetic dispersion originates from conformational substates and results in the observed distribution of primary CS rates, including fast activationless CS to  $P^+B_A^-$  in the majority of RCs, slightly activated, slow CS to  $P^+B_A^-$  in a minority of RCs, and superexchange-mediated CS to  $P^+H_A^-$  within this minority of RCs when the  $^1P^*$  lifetime is longer than 300 ps. As a characteristic spectral fingerprint, the reaction center minority performing slow CS shows a blue shift of  $230\text{ cm}^{-1}$  indicating a correlation of energetically lifted  $^1P^*$  states with stronger lifted  $P^+B_A^-$  states, which seems to originate from the interaction with charged amino acid residues in the vicinity of both P and  $B_A$ . In RCs of *Rb. sphaeroides* R26 we could trace conformational cooling of the state  $P^+H_A^-$  in the time window of one to several nanoseconds. Only a minor energetic stabilization is connected to this solvation process starting at about 0.20–0.22 eV below

$^1\text{P}^*$  and relaxing to values of 0.27 eV before  $\text{P}^+\text{H}_\text{A}^-$  decays owing to recombination.

**Acknowledgment.** It is a pleasure to acknowledge stimulating discussions with Prof. J. Jortner and Prof. M. Bixon. This work was supported by the Deutsche Forschungsgemeinschaft (SFB 143).

## References and Notes

- (1) *Protein Dynamics*, Eaton, W. A., Szabo, A., Eds.; *Chem. Phys.* (Special Issue) **1991**, 158, 191–531.
- (2) Frauenfelder, H.; Parak, F.; Young, R. D. *Annu. Rev. Biophys. Biochem.* **1988**, 17, 302.
- (3) Deisenhofer, J.; Epp, O.; Miki, K.; Huber, R.; Michel, H. *J. Mol. Biol.* **1984**, 180, 385.
- (4) Allen, J. P.; Feher, G.; Yeates, T. O.; Rees, D. C.; Deisenhofer, J.; Michel, H.; Huber, R. *Proc. Natl. Acad. Sci. U.S.A.* **1986**, 83, 8589.
- (5) Chang, C.-H.; Tiede, D.; Tang, J.; Smith, U.; Norris, J. R.; Schiffer, M. *FEBS Lett.* **1986**, 205, 82.
- (6) El Kabbani, O.; Chang, C. H.; Tiede, D.; Norris, J. R.; Schiffer, M. *Biochemistry* **1991**, 30, 5361.
- (7) Ermler, U.; Fritzsche, G.; Buchanan, S. K.; Michel, H. *Structure* **1994**, 2, 925.
- (8) Kirmaier, C.; Holten, D. In *The Photosynthetic Reaction Center*; Deisenhofer, J., Norris, J. R., Eds.; Academic: New York, 1993; p 49.
- (9) Breton, J.; Martin, J.-L.; Migus, A.; Antonetti, A.; Orszag, A. *Proc. Natl. Acad. Sci. U.S.A.* **1986**, 83, 5121.
- (10) Breton, J.; Martin, J.-L.; Petrich, J.; Migus, A.; Antonetti, A. *FEBS Lett.* **1986**, 209, 37.
- (11) Martin, J.-L.; Breton, J.; Hoff, A. J.; Migus, A.; Antonetti, A. *Proc. Natl. Acad. Sci. U.S.A.* **1986**, 83, 957.
- (12) Fleming, G. R.; Martin, J.-L.; Breton, J. *Nature* **1988**, 333, 190.
- (13) Du, M.; Rosenthal, S. J.; Xie, X.; DiMaggio, T. J.; Schmidt, M.; Hanson, D. K.; Schiffer, M.; Norris, J. R.; Fleming, G. R. *Proc. Natl. Acad. Sci. U.S.A.* **1992**, 89, 8517.
- (14) Vos, M. H.; Lambry, J.-C.; Robles, S.; Youvan, D. G.; Breton, J.; Martin, J.-L. *Proc. Natl. Acad. Sci. U.S.A.* **1991**, 88, 8885.
- (15) Müller, M. C.; Griebenow, K.; Holzwarth, A. R. *Chem. Phys. Lett.* **1992**, 199, 465.
- (16) Hamm, P.; Gray, K. A.; Oesterheld, D.; Feick, R.; Scheer, H.; Zinth, W.; *Biochim. Biophys. Acta* **1993**, 1142, 99.
- (17) Ogorodnik, A.; Keupp, W.; Volk, M.; Aumeier, G.; Michel-Beyerle, M. E. *J. Phys. Chem.* **1994**, 98, 3432.
- (18) Peloquin, J. M.; Williams, J. C.; Lin, X.; Alden, R. G.; Taguchi, A. K. W.; Allen, J. P.; Woodbury, N. W. *Biochemistry* **1994**, 33, 8098.
- (19) Hartwich, G.; Lossau, H.; Ogorodnik, A.; Michel-Beyerle, M. E. In *Reaction Centers of Photosynthetic Bacteria*; Michel-Beyerle, M. E., Ed.; Springer: Berlin, 1996; p 199.
- (20) Ogorodnik, A. *Mol. Cryst. Liq. Cryst.* **1993**, 230, 35.
- (21) Ogorodnik, A.; Michel-Beyerle, M. E. In *Photoprocesses in Transition Metal Complexes, Biosystems and Other Molecules. Experiment and Theory*; Kochanski, E., Ed.; Kluwer: Netherlands, 1992; p 349.
- (22) Keupp, W. Ph.D. Thesis, Technical University of Munich, 1994.
- (23) Schenck, C. C.; Blankenship, R. E.; Parson, W. W. *Biochim. Biophys. Acta* **1982**, 680, 44.
- (24) Woodbury, N. W.; Parson, W. W. *Biochim. Biophys. Acta* **1984**, 767, 345.
- (25) Hörber, J. K. H.; Göbel, W.; Ogorodnik, A.; Michel-Beyerle, M. E.; Cogdell, R. J. *FEBS Lett.* **1986**, 198, 273.
- (26) Woodbury, N. W.; Parson, W. W. *Biochim. Biophys. Acta* **1986**, 850, 197.
- (27) Ogorodnik, A.; Krüger, H. W.; Orthuber, H.; Haberkorn, R.; Michel-Beyerle, M. E.; Scheer, H. *Biophys. J.* **1982**, 39, 91.
- (28) Ogorodnik, A.; Volk, M.; Letterer, R.; Feick, R.; Michel-Beyerle, M. E. *Biochim. Biophys. Acta* **1988**, 936, 361.
- (29) Volk, M.; Ogorodnik, A.; Michel-Beyerle, M. E. In *Anoxygenic Photosynthetic Bacteria*; Blankenship, R. E., Madigan, M. T., Bauer, C. E., Eds.; Kluwer: Netherlands, 1995; p 595.
- (30) Ogorodnik, A. *Biochim. Biophys. Acta* **1990**, 1020, 65.
- (31) Woodbury, N. C.; Peloquin, J. M.; Alden, R. G.; Lin, X.; Lin, S.; Taguchi, A. K. W.; Williams, J. C.; Allen, J. P. *Biochemistry* **1994**, 33, 8101.
- (32) Holzwarth, A. R.; Müller, M. G. *Biochemistry* **1996**, 35, 11820.
- (33) Bixon, M.; Jortner, J.; Michel-Beyerle, M. E. *Chem. Phys.* **1995**, 197, 389.
- (34) Kaufmann, K. J.; Petty, K. M.; Dutton, P. L.; Renzepis, P. M. *Biochem. Biophys. Res. Commun.* **1976**, 70, 839.
- (35) Holten, D.; Hoganson, C.; Windsor, M. W.; Schenck, C. C.; Parson, W. W.; Migus, A.; Fork, R. L.; Shank, C. V. *Biochim. Biophys. Acta* **1980**, 592, 461.
- (36) Kirmaier, C.; Holten, D. *Proc. Natl. Acad. Sci. U.S.A.* **1990**, 87, 3552.
- (37) Feher, G.; Okamura, M. Y. In *The Photosynthetic Bacteria*; Clayton, R. K., Sistrom, W. R., Eds.; Plenum: New York 1978; p 349.
- (38) Gunner, M. R.; Robertson, D. E.; Dutton, P. L. *J. Phys. Chem.* **1986**, 90, 3783.
- (39) Volk, M.; Aumeier, G.; Häberle, T.; Ogorodnik, A.; Feick, R.; Michel-Beyerle, M. E. *Biochim. Biophys. Acta* **1992**, 1102, 253.
- (40) Bevington, P. R.; Robinson, D. K. *Data Reduction and Error Analysis for the Physical Science*, 2nd ed.; McGraw-Hill International: New York, 1992.
- (41) Schmidt, S.; Arlt, T.; Hamm, P.; Lauterwasser, C.; Finkle, U.; Drews, G.; Zinth, W. *Biochim. Biophys. Acta* **1993**, 1144, 385.
- (42) Xiao, W.; Lin, S.; Taguchi, A. K. W.; Woodbury, N. W. *Biochemistry* **1994**, 33, 8313.
- (43) Müller, M. G.; Drews, G.; Holzwarth, A. *Chem. Phys. Lett.* **1996**, 258, 194.
- (44) Owing to the limited time resolution of our setting (40 ps fwhm) only the relative quantum yield for the fast prompt fluorescence is used to adapt the fitting curve to the decay trace within the instrumental response function. Thus, a slightly increased  $\tau_1$  value for  $\text{Q}_\text{A}$ -free RC relative to  $\tau_1$  for  $\text{Q}_\text{A}$ -containing RC would result in an increase of the amplitudes  $a_2$  to  $a_5$  for  $\text{Q}_\text{A}$ -free RC by the factor  $\tau_1(\text{Q}_\text{A}\text{-free RC})/\tau_1(\text{Q}_\text{A}\text{-containing RC})$ .
- (45) Lossau, H. Ph.D. Thesis, Technical University of Munich, 1998.
- (46) Jia, Y.; DiMaggio, T. J.; Chan, C.-K.; Wang, Z.; Du, M.; Hanson, D. K.; Schiffer, M.; Norris, J. R.; Fleming, G. R.; Popov, M. S. *J. Phys. Chem.* **1993**, 97, 13180.
- (47) Arlt, T.; Schmidt, S.; Kaiser, W.; Lauterwasser, C.; Meyer, M.; Scheer, H.; Zinth, W. *Proc. Natl. Acad. Sci. U.S.A.* **1993**, 90, 11757.
- (48) Holzappel, W.; Finkle, U.; Kaiser, W.; Oesterheld, D.; Scheer, H.; Stütz, H. U.; Zinth, W. *Proc. Natl. Acad. Sci. U.S.A.* **1990**, 87, 5168.
- (49) Vos, M. H.; Lambry, J.-C.; Robles, S. J.; Youvan, D. C.; Breton, J.; Martin, J.-L. *Proc. Natl. Acad. Sci. U.S.A.* **1992**, 89, 613.
- (50) Chan, C. K.; DiMaggio, T. J.; Chen, L. X. Q.; Norris, J. R.; Fleming, G. R. *Proc. Natl. Acad. Sci. U.S.A.* **1991**, 88, 11202.
- (51) Robles, S. J.; Breton, J.; Youvan, D. C. *Science* **1990**, 248, 1402.
- (52) Breton, J.; Martin, J.-L.; Lambry, J.-C.; Robles, S. J.; Youvan, D. C. In *Reaction Centers of Photosynthetic Bacteria*; Michel-Beyerle, M. E., Ed.; Springer: Berlin, 1990; p 293.
- (53) Eberl, U.; Gilbert, M.; Keupp, W.; Langenbacher, T.; Siegl, J.; Sinning, I.; Ogorodnik, A.; Robles, S. J.; Breton, J.; Youvan, D. C.; Michel-Beyerle, M. E. In *The Photosynthetic Bacterial Reaction Center*; Breton, J., Vermeglio, A., Eds.; Plenum: New York, 1992; p 253.
- (54) Müller, P.; Bieser, G.; Hartwich, G.; Langenbacher, T.; Ogorodnik, A.; Michel-Beyerle, M.-E. *Ber. Bunsen-Ges. Phys. Chem.* **1996**, 100, 1967.
- (55) Lockhart, D. J.; Goldstein, R. F.; Boxer, S. G. *J. Chem. Phys.* **1988**, 89, 1409.
- (56) Ogorodnik, A.; Eberl, U.; Heckmann, R.; Kappl, M.; Feick, R.; Michel-Beyerle, M. E. *J. Phys. Chem.* **1991**, 95, 2036.
- (57) Eberl, U. Ph.D. Thesis, Technical University of Munich, 1992.
- (58) Eberl, U.; Ogorodnik, A.; Michel-Beyerle, M. E. *Z. Naturforsch.* **1990**, 45a, 763–770.
- (59) Though it is rather unlikely, one cannot rule out completely that a very large electric field effect on the small contribution from delayed emission of  $\text{P}^+\text{H}_\text{A}^-$  of  $\approx 10\%$   $\text{Q}_\text{A}$ -depleted RCs being present in the samples of refs 20–22 could dominate the overall electric field effect. The quantum yields of the 850 ps and 5.2 ns fluorescence components are clearly larger than those of the highly  $\text{Q}_\text{A}$ -reconstituted samples investigated in this work. Furthermore the relative field effects increase significantly with time, i.e., concomitantly with the relative increase of the delayed emission. In refs 20, 21, 57, and 58 the weak dependence of the effect on the magnitude of the electric field has been taken as additional evidence against a dominant contribution of delayed emission. It is quadratic up to the highest fields applied, while an exponential dependence is expected for the delayed emission. This argument, however, does not hold any longer, since an energetic inhomogeneity was found on  $\text{P}^+\text{H}_\text{A}^-$  being as large as the field-induced energy shifts, so that the field effect is reduced significantly. A comparative study of the field effects of  $\text{Q}_\text{A}$ -depleted and -reconstituted samples—analogueous to the comparison presented in this paper—would be necessary for a ponderable assignment of the observed electric field effects to prompt or delayed emission.
- (60) Bixon, M.; Jortner, J.; Michel-Beyerle, M. E. *Biochim. Biophys. Acta* **1991**, 1056, 301.
- (61) Bixon, M.; Jortner, J.; Michel-Beyerle, M. E. *Chem. Phys.* **1995**, 197, 389.
- (62) Lin, S.; Taguchi, A. K. W.; Woodbury, N. W. *J. Phys. Chem.* **1996**, 100, 17067.
- (63) Peloquin, J. M.; Lin, S.; Taguchi, A. K. W.; Woodbury, N. W. *J. Phys. Chem.* **1995**, 99, 1349.